JOURNAL OF COMPUTATIONAL PHYSICS **147,** 485–506 (1998)
ARTICLE NO. CP986098

An Iterative Method for the Inversion of the Two-Dimensional Wave Equation with a Potential[1]

Guanquan Zhang* and Yu Zhang*,†,[2]

*State Key Laboratory of Scientific and Engineering Computing, Institute of Computational Mathematics and Scientific/Engineering Computing, Chinese Academy of Sciences, Beijing, 100080 People's Republic of China; †Applied Mathematics Department, 217-50, California Institute of Technology, Pasadena, California 91125
E-mail: zgq@lsec.cc.ac.cn, zyu@ama.caltech.edu

Received October 23, 1997; revised September 9, 1998

A numerical method for a nonlinear inversion problem for the 2D wave equation with a potential is discussed. In order to avoid the ill-posedness, we substitute a coupled system of one-way wave equations for the original wave equation. An iterative algorithm is constructed to improve the accuracy of the inversion. Numerical experiments are performed on several examples to examine the effectiveness of this method.

Key Words: ill-posedness; nonlinear inversion; wave splitting.

1. INTRODUCTION

In this paper, we describe a numerical nonlinear inversion method for recovering the potential $v(x, z)$ in the two-dimensional plasma wave equation from the boundary response of the half-plane $z > 0$ excited by an impulsive line source. That is, we consider

$$\begin{aligned}
\left[\frac{\partial^2}{\partial t^2} - \frac{\partial^2}{\partial x^2} - \frac{\partial^2}{\partial z^2} + v(x, z)\right] p(t, x, z) &= 0, && z > 0, t > 0,\\
p(0, x, z) = \frac{\partial}{\partial t} p(0, x, z) &= 0, && z > 0,\\
p(t, x, 0) &= \delta(t), && t \geq 0,\\
\frac{\partial}{\partial z} p(t, x, 0) &= h(t, x), && t \geq 0,
\end{aligned} \tag{1.1}$$

[1] Supported by China State Major Key Project for Basic Research.

[2] Corresponding author.

0021-9991/98 $25.00

and seek to determine the unknown potential $v(x, z)$ from the response $h(t, x)$. This problem has several applications. We refer readers to the discussion in [22] for further references. What motivates us to study this problem is its application to petroleum prospecting in reconstructing an acoustic medium with density and wave speed from surface measurements of the displacement response to a line source. In one dimension, the corresponding inverse problem is well-posed and has been investigated both theoretically and numerically (see [17, 12, 3, 4, 11, 25, 19]). But in higher dimensions, like inverse problems of other multidimensional hyperbolic equations, very little is known. The main difficulties lie in the nonlinearity and ill-posedness.

Due to the stimulation of applications in many fields, such as seismic prospecting, medical imaging, nondestructive testing, radar detection, etc., inverse problems in multidimensional wave equations have attracted remarkable research interests in past decades. Various methods based on linearization or optimization (for example, [18, 6]) are discussed and developed; however, good directly nonlinear inversion methods are still under development. We refer readers to the survey papers [1, 10]. In [21], Yagle and Levy suggested a layer-stripping method for the inverse problem (1.1) and in [22] Yagle and Raadhakrishnan presented the results of some numerical experiments. Their main idea is to regularize the ill-posed problem by cutting the lateral wave numbers. In contrast, our approach for regularizing the problem is based on the wave splitting method developed by Zhang in [23, 24, 27]. By splitting the wave field into upgoing waves $U(t, x, z)$ and downgoing waves $D(t, x, z)$ which are governed by pseudo-differential equations, the nonradiative wave, which causes the ill-posedness, is naturally regularized. As proved in [23], the derived one-way wave equations are well-posed when the reference spatial direction is treated as the evolution direction. Therefore, using the relation on the characteristic

$$U(z+, x, z) = -\frac{1}{2}v(x, z), \tag{1.2}$$

derived by causality, $v(x, z)$ can be stably solved layer by layer as a nonlinear initial value problem in the z direction.

Since the early seventies, one-way wave equations have been applied to geophysical exploration. Usually, one considers the response as the primary reflection and uses the decoupled upgoing one-way wave equation to extrapolate the upgoing wave field from the response recorded on the surface, downward towards the interior of the earth. Additionally, this extrapolation picks out the upgoing wave at each point at the arrival time of the downgoing wave to image the underground structure. Such a technique is called migration ([16]). In migration the multireflection is considered to be noise. The main difference between the inversion method discussed in this paper and the migration method is that all reflections, not only the primary reflection, but also the multiple reflections, are taken into consideration. So migration is regarded as a linearized inversion, which can also be considered as the first order approximation of the full nonlinear inversion developed in this paper.

This paper can be regarded as the continuation of the work in [13, 28]. Some modifications are made to the derived one-way wave equations and their initial and boundary conditions, high-order approximations are used in the numerical inversion and an iterative inversion algorithm is constructed. With these modifications, the numerical results are remarkably improved.

This paper is organized as follows. In Section 2, we introduce the wave-splitting technique and derive the one-way wave equations and their approximations for the propagation

operator. In Section 3, we discuss the inverse problem for the system of coupled one-way wave equations and their initial and boundary conditions. Unlike the original inverse problem, it is well-posed and can be solved by the layer stripping method. In Section 4, we introduce the finite difference schemes and the numerical implementation for the inverse problem discussed in Section 3. In Section 5, we construct an iterative algorithm to improve the inversion accuracy. Finally, we present several numerical examples in Section 6.

2. SPLITTING OF WAVE FIELDS

Splitting of wave fields is not new, many researchers have studied it with various approaches. Weston *et al.* worked on splitting and derived a coupled differential-integral system [20]. Fishman studied splitting by the Weyl pseudo-differential operator [9]. Our approach to wave splitting is close to the method proposed by Engquist and Majda in [8] which was originally used to deal with the absorbing boundary conditions.

First, we consider the two-dimensional propagation operator

$$\frac{\partial^2}{\partial t^2} - \frac{\partial^2}{\partial x^2} - \frac{\partial^2}{\partial z^2}, \tag{2.1}$$

with dispersion relation

$$ik_z = \pm ik_t\sqrt{1 - k_x^2/k_t^2}. \tag{2.2}$$

We rewrite the operator (2.1) as

$$\frac{\partial^2}{\partial t^2} - \frac{\partial^2}{\partial x^2} - \frac{\partial^2}{\partial z^2} = \left(\Lambda + \frac{\partial}{\partial z}\right)\left(\Lambda - \frac{\partial}{\partial z}\right). \tag{2.3}$$

Here, Λ is called a square-root operator and can be regarded as a pseudo-differential operator with the symbol

$$\lambda = ik_t\sqrt{1 - k_x^2/k_t^2}. \tag{2.4}$$

We seek an approximation operator Λ_n to Λ. For the sake of simplicity and clearness, we ignore the rigorous discussion of pseudo-differential operators in the following deduction and will come back to explain the meaning of the operator Λ.

In Appendix A, we prove the following proposition.

PROPOSITION 1. *For all the complex numbers $\xi \notin (-\infty, -1) \cup (1, +\infty)$, the following integral equality*

$$\sqrt{1 - \xi^2} = 1 - \frac{\xi^2}{\pi}\int_{-1}^{1} \frac{\sqrt{1 - s^2}}{1 - \xi s}\, ds \tag{2.5}$$

is valid.

Using Eq. (2.5), the symbol λ can be expressed as

$$\lambda = ik_t - \frac{i}{\pi}\int_{-1}^{1} \sqrt{1 - s^2}\frac{k_x^2}{k_t - sk_x}\, ds \quad \text{when } \left|\frac{k_x}{k_t}\right| < 1. \tag{2.6}$$

For real r, define

$$I(r) := \frac{1}{r}\left[1 - \sqrt{1 - r^2}\right]. \tag{2.7}$$

Then by the definition (2.4) of λ, the function $I(r)$ and symbol λ have the relation

$$\lambda = ik_t - ik_x I\left(\frac{k_x}{k_t}\right). \tag{2.8}$$

By discretizing (2.5), it is easy to see that when $|r| < 1$, $I(r)$ can be approximated by the rational function $I_n(r)$,

$$I_n(r) = \sum_{l=1}^{n} \frac{a_{n,l} r}{1 - \alpha_{n,l} r}, \tag{2.9}$$

where

$$a_{n,l} = \frac{1}{n+1} \sin^2\left(\frac{l\pi}{n+1}\right), \tag{2.10}$$

$$\alpha_{n,l} = \cos\left(\frac{l\pi}{n+1}\right), \tag{2.11}$$

and the approximation order is

$$I(r) - I_n(r) = O(r^{2n+1}). \tag{2.12}$$

See [23] for a rigorous proof. Combining (2.8) and (2.9), we get the approximations to the symbol λ,

$$\lambda_n := ik_t - ik_x I_n\left(\frac{k_x}{k_t}\right) = ik_t - ik_x^2 \sum_{l=1}^{n} \frac{a_{n,l}}{k_t - \alpha_{n,l} k_x}. \tag{2.13}$$

Using the correspondence

$$ik_t \leftrightarrow \frac{\partial}{\partial t}, \quad ik_x \leftrightarrow \frac{\partial}{\partial x}, \tag{2.14}$$

returning to the t-x domain, and using (2.6), the square-root operator Λ can be written as

$$\Lambda = \frac{\partial}{\partial t} - R, \tag{2.15}$$

where I is the identity operator, R is a pseudo-differential operator defined as

$$R[p(t,x,z)] := \frac{1}{\pi} \int_{-1}^{1} \sqrt{1 - s^2}\, q(s;t,x,z)\, ds, \tag{2.16}$$

and the auxiliary function $q(s;t,x,z)$ satisfies

$$\left(\frac{\partial}{\partial t} - s\frac{\partial}{\partial x}\right) q(s;t,x,z) = \frac{\partial^2}{\partial x^2} p(t,x,z). \tag{2.17}$$

If we define U and D as

$$U := \left[\frac{\partial}{\partial t} - R + \frac{\partial}{\partial z}\right] p, \tag{2.18}$$

$$D := \left[\frac{\partial}{\partial t} - R - \frac{\partial}{\partial z}\right] p, \tag{2.19}$$

respectively, then the wave equation

$$\left(\frac{\partial^2}{\partial t^2} - \frac{\partial^2}{\partial x^2} - \frac{\partial^2}{\partial z^2}\right) p(t, x, z) = 0 \tag{2.20}$$

is replaced by the system of one-way wave equations,

$$\begin{aligned} &\left(\frac{\partial}{\partial t} - \frac{\partial}{\partial z}\right) U - \frac{1}{\pi} \int_{-1}^{1} \sqrt{1 - s^2}\, q_U(s; t, x, z)\, ds = 0, \\ &\left(\frac{\partial}{\partial t} + \frac{\partial}{\partial z}\right) D - \frac{1}{\pi} \int_{-1}^{1} \sqrt{1 - s^2}\, q_D(s; t, x, z)\, ds = 0, \\ &\frac{\partial}{\partial z} p = \frac{U - D}{2}, \end{aligned} \tag{2.21}$$

where q_U and q_D satisfy

$$\left(\frac{\partial}{\partial t} - s\frac{\partial}{\partial x}\right) \begin{pmatrix} q_U(s; t, x, z) \\ q_D(s; t, x, z) \end{pmatrix} = \frac{\partial^2}{\partial x^2} \begin{pmatrix} U(t, x, z) \\ D(t, x, z) \end{pmatrix}. \tag{2.22}$$

The planar waves $f(t - (\alpha z + \beta x))$ and their superpositions are solutions of the wave equation (2.20) if f is twice differentiable, and $\alpha^2 + \beta^2 = 1$. It is easy to verify that for all $\alpha \le 0$ ($\alpha \ge 0$), the planar waves $f(t - (\alpha z + \beta x))$ and their superpositions satisfy the one-way wave equation for U (D) in (2.21). In geophysical applications, the variable z is used to represent the depth under the surface of the earth, so we designate $U(t, x, z)$ the upgoing wave and $D(t, x, z)$ the downgoing wave.

One question naturally arises for the splitting wave equation system (2.21): In what sense does it simulate the original equation (2.20)? First, such wave splitting is accurate for the one-dimensional case ([25]). Second, in [27], the author proved that the coupled system (2.21) and the wave equation (2.20) are equivalent in the sense of high-frequency approximation (geometrical optic approximation). Both have the same eikonal equation and the same first transport equation; that is, system (2.21) preserves the kinetic and dynamic properties of the original wave equation. Third, due to Eq. (2.6), such wave splitting is only valid for the radiative wave, where $|k_x/k_t| < 1$. For real k_x, k_t and $|k_x/k_t| > 1$, λ is taken to be zero (see Remark 2). We remind readers that it is the nonradiative wave ($|k_x/k_t| > 1$) which causes the ill-posedness in solving the spatial initial problem. Therefore by reformulating the wave equation, we have actually regularized the problem.

Remark 1. In [27], the author obtained a general approximate splitting formulation for

$$\left(\frac{1}{c(x, z)^2}\frac{\partial^2}{\partial t^2} - \frac{\partial^2}{\partial x^2} - \frac{\partial^2}{\partial z^2}\right) p = 0, \tag{2.23}$$

as

$$\begin{aligned}
&\left(\frac{1}{c}\frac{\partial}{\partial t}-\frac{\partial}{\partial z}\right)U-\frac{1}{c}\frac{\partial}{\partial t}\left[\frac{1}{\pi}\int_{-1}^{1}\sqrt{1-s^2}\,q_U^c(s;t,x,z)\,ds\right]\\
&\quad+\frac{c_z}{2c}\left[D+U+q_U^c(1;t,x,z)+q_D^c(1;t,x,z)\right]=0,\\
&\left(\frac{1}{c}\frac{\partial}{\partial t}+\frac{\partial}{\partial z}\right)D-\frac{1}{c}\frac{\partial}{\partial t}\left[\frac{1}{\pi}\int_{-1}^{1}\sqrt{1-s^2}\,q_D^c(s;t,x,z)\,ds\right]\\
&\quad+\frac{c_z}{2c}\left[D+U+q_U^c(1;t,x,z)+q_D^c(1;t,x,z)\right]=0,
\end{aligned}\tag{2.24}$$

where q_U^c and q_D^c satisfy

$$\left(\frac{\partial^2}{\partial t^2}-s^2\left(c\frac{\partial}{\partial x}\right)^2\right)\begin{pmatrix}q_U^c(s;t,x,z)\\ q_D^c(s;t,x,z)\end{pmatrix}=\left(c\frac{\partial}{\partial x}\right)^2\begin{pmatrix}U(t,x,z)\\ D(t,x,z)\end{pmatrix}.\tag{2.25}$$

The above discussion is also valid for splitting (2.24) even when $c(x,z)$ is piecewisely smooth.

Remark 2. If we define

$$I(r):=\lim_{\varepsilon\to 0}\mathrm{Re}\left(\frac{r+\varepsilon i}{\pi}\int_{-1}^{1}\frac{\sqrt{1-s^2}}{1-(r+\varepsilon i)s}\,ds\right),$$

by Proposition 1, we have

$$\lambda:=ik_t-ik_xI\left(\frac{k_x}{k_t}\right)=\begin{cases}ik_t\sqrt{1-\frac{k_x^2}{k_t^2}}, & \left|\frac{k_x}{k_t}\right|<1,\\ 0, & \left|\frac{k_x}{k_t}\right|>1.\end{cases}\tag{2.26}$$

Remark 3. In [29], we proved that if $p(t,x,z)$ is a solution of wave equation (2.20) with L_1 integrable initial time conditions, then the support of Fourier transform for its response $\hat{p}(k_t,k_x,z=0)$ must be contained in $\Omega=\{(k_t,k_x):|k_t|\geq|k_x|\}$; i.e., the response at $z=0$ does not contain the nonradiative part. But for the variable coefficient wave equation (2.23) or (1.1), such a conclusion is no longer true, and thus the splitting is incomplete.

In numerical computations, it is convenient to use the approximate splitting system instead of system (2.21). From the approximate symbol λ_n defined by (2.13), we obtain

$$\begin{aligned}
&\left(\frac{\partial}{\partial t}-\frac{\partial}{\partial z}\right)U-\sum_{l=1}^{n}a_{n,l}q_U(\alpha_{n,l};t,x,z)=0,\\
&\left(\frac{\partial}{\partial t}+\frac{\partial}{\partial z}\right)D-\sum_{l=1}^{n}a_{n,l}q_D(\alpha_{n,l};t,x,z)=0,\\
&\frac{\partial}{\partial z}p=\frac{U-D}{2}.
\end{aligned}\tag{2.27}$$

Unlike the original equation (2.20), the z-direction initial value problem for (2.27) is well-posed; see [23] or [29].

Remark 4. The first equation for U in (2.27) has been used in migration (see [24]). The special cases for $n=1$ and $n=2$ are classical 15° ([5]) and 40° ([15] or [2]) migration equations which are widely used in seismic exploration. In general, one-way wave equations (2.27) are $d(n)$ degree equations, where $d(n)$ is an increasing function of n and $\lim_{n\to\infty} d(n) = 90^\circ$.

Remark 5. The wave splitting technique discussed here can be generalized to the three spatial dimension wave operator. The symbol for the 3D square-root operator is

$$\lambda = ik_t\sqrt{1-\left(k_x^2+k_y^2\right)/k_t^2}. \tag{2.28}$$

Using (2.5)

$$\sqrt{1-\xi^2} = 1-\frac{\xi^2}{\pi}\int_{-1}^{1}\frac{\sqrt{1-s^2}}{1-\xi s}\,ds = 1-\frac{\xi^2}{\pi}\int_{-1}^{1}\frac{\sqrt{1-s^2}}{1-\xi^2 s^2}\,ds, \tag{2.29}$$

λ can be expressed as

$$\lambda = ik_t\left(1-\frac{k_x^2+k_y^2}{\pi}\int_{-1}^{1}\frac{\sqrt{1-s^2}}{k_t^2-\left(k_x^2+k_y^2\right)s^2}\,ds\right), \quad k_x^2+k_y^2 < k_t^2, \tag{2.30}$$

and the the approximate symbols λ_n are

$$\lambda_n = ik_t\left[1-\sum_{l=1}^{n}\frac{a_{n,l}\left(k_x^2+k_y^2\right)}{k_t^2-\alpha_{n,l}\left(k_x^2+k_y^2\right)}\right]. \tag{2.31}$$

From (2.30) and (2.31), it is easy to derive the one-way wave equations and their approximate equations for the 3D case.

3. INVERSE PROBLEM FOR THE SYSTEM OF COUPLED ONE-WAY WAVE EQUATIONS

Applying the square-root operator introduced in Section 2, the inverse problem (1.1) can be reformulated as

$$\begin{gathered}
\left(\frac{\partial}{\partial t}-\frac{\partial}{\partial z}\right)U-\frac{1}{\pi}\int_{-1}^{1}\sqrt{1-s^2}\,q_U(s;t,x,z)\,ds+vp=0,\\
\left(\frac{\partial}{\partial t}+\frac{\partial}{\partial z}\right)D-\frac{1}{\pi}\int_{-1}^{1}\sqrt{1-s^2}\,q_D(s;t,x,z)\,ds+vp=0,\\
\frac{\partial}{\partial z}p=\frac{U-D}{2},\\
\left(\frac{\partial}{\partial t}-s\frac{\partial}{\partial x}\right)\begin{pmatrix}q_U(s;t,x,z)\\ q_D(s;t,x,z)\end{pmatrix}=\frac{\partial^2}{\partial x^2}\begin{pmatrix}U(t,x,z)\\ D(t,x,z)\end{pmatrix},\\
U(t,x,0)=-D(t,x,0)=h(t,x),\\
p(t,x,0)=\delta(t).
\end{gathered} \tag{3.1}$$

System (3.1) is nonlinear and coupled because of the term vp. In this system, all the multiple reflections are taken into consideration. When the response $h(t, x)$ is small, D, U, p, and v are also small. If we drop the high order term vp, system (3.1) is reduced to the linear and decoupled system (2.21). The first equation of (2.21) is the basic upcoming one-way wave equation, which is used in migration. So migration can be considered as the linearized first order approximation of the full nonlinear inverse problem discussed in this section.

From propagation theory, the δ singularity will be propagated along the surface $t = z$ which is the envelope of the characteristic cones with vertices on the x-axis. Singularity propagation analysis for (3.1) (see [13] or [7]) yields the values of U and D on $t = z$,

$$U(z+, x, z) = -\frac{1}{2}v(x, z), \tag{3.2}$$

$$q_U(s; z+, x, z) = 0, \tag{3.3}$$

and

$$D(z+, x, z) = \int_0^z \left[\frac{\partial^2}{\partial t^2} - v(x, \xi)\right] g(x, \xi)\, d\xi - h(0+, x), \tag{3.4}$$

$$q_D(z+, x, z) = 0, \tag{3.5}$$

where

$$g(x, z) = -\frac{1}{2}\int_0^z v(x, \xi)\, d\xi.$$

Remark 1. For the original inverse problem (1.1), we can also obtain the following conditions for p by singularity propagation analysis, which were used to construct the layer-stripping algorithm in [22],

$$\left(\frac{\partial}{\partial t} + \frac{\partial}{\partial z}\right) p(t = z+, x, z) = -\frac{v(x, z)}{2},$$

$$\left(\frac{\partial}{\partial t} - \frac{\partial}{\partial z}\right) p(t = z+, x, z) = \int_0^z \left[\frac{\partial^2}{\partial t^2} - v(x, \xi)\right] g(x, \xi)\, d\xi - h(0+, x).$$

Similar to (2.27), we use the approximate coupled system in numerical computations,

$$\begin{aligned}
&\left(\frac{\partial}{\partial t} - \frac{\partial}{\partial z}\right) U - \sum_{l=1}^{n} a_{n,l} q_U(\alpha_{n,l}) + vp = 0,\\
&\left(\frac{\partial}{\partial t} + \frac{\partial}{\partial z}\right) D - \sum_{l=1}^{n} a_{n,l} q_D(\alpha_{n,l}) + vp = 0,\\
&\frac{\partial}{\partial z} p = \frac{U - D}{2},\\
&\left(\frac{\partial}{\partial t} - \alpha_{n,l}\frac{\partial}{\partial x}\right)\begin{pmatrix} q_U(\alpha_{n,l}; t, x, z) \\ q_D(\alpha_{n,l}; t, x, z)\end{pmatrix} = \frac{\partial^2}{\partial x^2}\begin{pmatrix} U(t, x, z) \\ D(t, x, z)\end{pmatrix}.
\end{aligned} \tag{3.6}$$

In order to solve (3.6), initial and boundary conditions must be added. According to the

original problem (1.1), at the surface $z = 0$ for $t > 0$,

$$\begin{aligned} U(t, x, 0) &= h(t, x), \\ D(t, x, 0) &= -h(t, x), \quad \text{for } t > 0, \\ p(t, x, 0) &= 0. \end{aligned} \tag{3.7}$$

Along $t = z$, we use the results of singularity propagation analysis for D and q_D

$$\begin{aligned} D(z, x, z) &= \int_0^z \left[\frac{\partial^2}{\partial t^2} - v(x, \xi) \right] g(x, \xi)\, d\xi - h(0+, x), \\ q_D(\alpha_{n,l}, t, x, z) &= 0, \quad l = 1, \ldots, n. \end{aligned} \tag{3.8}$$

For the sake of stability and closeness, some kind of large-time conditions must be proposed for U and q_U, for example, for large T

$$\begin{aligned} U(T, x, z) &= 0, \\ q_U(\alpha_{n,l}; T, x, z) &= 0, \quad l = 1, \ldots, n. \end{aligned} \tag{3.9}$$

Finally, we use the following relationship to reconstruct the potential $v(x, z)$:

$$v(x, z) = -2U(z, x, z). \tag{3.10}$$

The inverse problem for the one-way wave equation system (3.6)–(3.10) can be solved in the domain $\Omega = \{(t, x, z) : x \in R, t \geq z > 0\}$ by the well-known layer-stripping algorithm. We discuss its numerical implementation in the next section.

Remark 2. Among all the conditions proposed above, the large-time conditions (3.9) do not seem to be very reasonable. When $v(x, z)$ is compactly supported, the upgoing wave U satisfies

$$\lim_{t \to \infty} U(t, x, z) = 0. \tag{3.11}$$

The first condition in (3.9) can be regarded as an approximation to (3.11) when T is very large. In practice, T cannot be very large; otherwise, a long record of the response $h(t, x)$ is required and the computational effort increases. Numerical tests tell us that the large-time conditions affect the accuracy of inversion and need to be further studied. In numerical inversions, we use the approximate conditions instead of (3.9):

$$\begin{aligned} U(T, x, z) &= -D(T, x, z), \\ q_U(\alpha_{n,l}; T, x, z) &= -q_D(\alpha_{n,l}; T, x, z), \quad l = 1, \ldots, n. \end{aligned} \tag{3.12}$$

From conditions (3.7), (3.12) is valid at $z = 0$ and can be regarded as approximate conditions when $z > 0$. From numerical experiments, it seems that such conditions work well even when T is not very large (see the numerical examples in Section 6).

Remark 3. The inversion method discussed in this paper can be easily generalized to the 3D case; see Remark 5 in Section 2.

Remark 4. For the inverse acoustical wave problem with variable velocity

$$\begin{aligned}\left[\frac{1}{c(x,z)^2}\frac{\partial^2}{\partial t^2}-\frac{\partial^2}{\partial x^2}-\frac{\partial^2}{\partial z^2}\right]p(t,x,z)&=0, \qquad z>0, t>0,\\ p(0,x,z)=\frac{\partial}{\partial t}p(0,x,z)&=0, \qquad z>0,\\ p(t,x,0)&=\delta(t), \qquad t\geq 0,\\ \frac{\partial}{\partial z}p(t,x,0)&=h(t,x), \quad t\geq 0;\end{aligned} \tag{3.13}$$

a similar inversion method was suggested in [26].

4. NUMERICAL IMPLEMENTATION OF THE INVERSE PROBLEM FOR THE SYSTEM OF COUPLED ONE-WAY WAVE EQUATIONS

In this section we describe the difference scheme for the 2D layer-stripping algorithm for the solution of the inverse problem (3.6)–(3.8), (3.12), and (3.10).

Let Ω be the domain $\Omega=\{(t,x,z)\,|\,t\geq z\}$, and cover Ω by the grid $\{(t_i,x_j,z_k)\,|\,t_i=i\cdot\Delta t, x_j=j\cdot\Delta x, z_k=k\cdot\Delta z, \Delta t=\Delta z=\Delta$, on grid points $j+k=$ even number$\}$, shown in Fig. 1. Denoting $f^i_{j,k}=f(t_i,x_j,z_k)$, and discretizing equations (3.6) along the characteristic direction $t+z=c_1$, $t-z=c_2$, we obtain

$$\frac{U^j_{i,k}-U^j_{i-1,k+1}}{\Delta}-\sum_{l=1}^{n}a_{n,l}(q_U(\alpha_{n,l}))^j_{i-1/2,k+1/2}+v^j_{k+1/2}p^j_{i-1/2,k+1/2}=0, \tag{4.1}$$

$$\frac{D^j_{i,k}-D^j_{i-1,k-1}}{\Delta}-\sum_{l=1}^{n}a_{n,l}(q_D(\alpha_{n,l}))^j_{i-1/2,k-1/2}+v^j_{k-1/2}p^j_{i-1/2,k-1/2}=0, \tag{4.2}$$

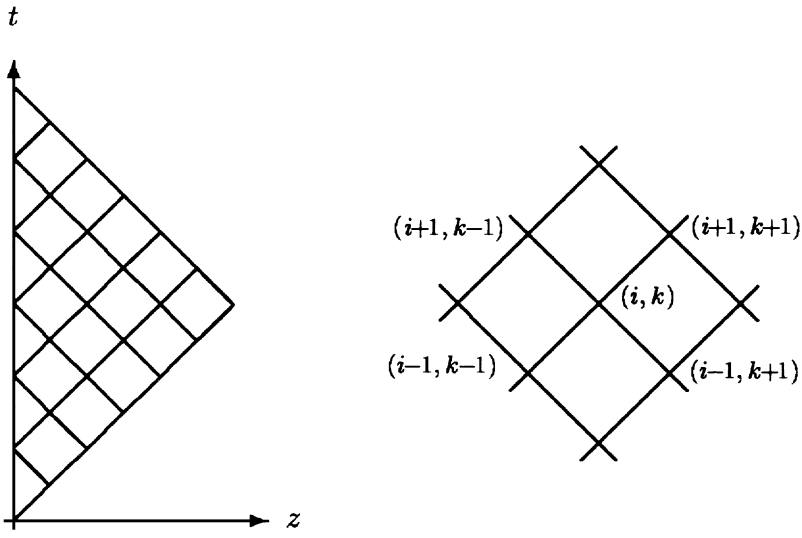

FIG. 1. The grid used in numerical computation.

$$\frac{p^j_{i,k}-p^j_{i,k-1}}{\Delta}=\frac{1}{4}\big(U^j_{i,k-1}+U^j_{i,k}-D^j_{i,k-1}-D^j_{i,k}\big), \tag{4.3}$$

$$\begin{aligned}&\frac{(q_U(\alpha_{n,l}))^j_{i+3/2,k+1/2}-(q_U(\alpha_{n,l}))^j_{i-1/2,k+1/2}}{2\Delta}\\&\quad-\alpha_{n,l}\frac{\Delta_x}{4\Delta x}\big(q_U(\alpha_{n,l}))^j_{i+3/2,k+1/2}+(q_U(\alpha_{n,l}))^j_{i-1/2,k+1/2}\big)\\&\quad=\frac{\Delta_x^2}{4\Delta x^2}\big(U^j_{i,k}+U^j_{i-1,k+1}+U^j_{i+2,k}+U^j_{i+1,k+1}\big),\end{aligned} \tag{4.4}$$

$$\begin{aligned}&\frac{(q_D(\alpha_{n,l}))^j_{i-1/2,k-1/2}-(q_D(\alpha_{n,l}))^j_{i-5/2,k-1/2}}{2\Delta}\\&\quad-\alpha_{n,l}\frac{\Delta_x}{4\Delta x}\big(q_D(\alpha_{n,l}))^j_{i-1/2,k-1/2}+(q_D(\alpha_{n,l}))^j_{i-5/2,k-1/2}\big)\\&\quad=\frac{\Delta_x^2}{4\Delta x^2}\big(D^j_{i,k}+D^j_{i-1,k-1}+D^j_{i-2,k}+D^j_{i-3,k-1}\big),\end{aligned} \tag{4.5}$$

where

$$\Delta_x f(x)=f(x+\Delta x)-f(x-\Delta x), \tag{4.6}$$

$$\Delta_x^2 f(x)=f(x+\Delta x)-2f(x)+f(x-\Delta x), \tag{4.7}$$

$$v^j_{k+1/2}=\frac{v^j_{k+1}+v^j_k}{2}, \tag{4.8}$$

$$p^j_{i,k-1/2}=\frac{p^j_{i,k}+p^j_{i,k-1}}{2}. \tag{4.9}$$

The above difference schemes, (4.1)–(4.5), are implicit and have second-order truncation errors. To simplify the algorithm, we first use the explicit difference schemes for the auxiliary functions $q_U(\alpha_{n,l})$ and $q_D(\alpha_{n,l})$:

$$\begin{aligned}&\frac{(q_U(\alpha_{n,l}))^j_{i+3/2,k+1/2}-(q_U(\alpha_{n,l}))^j_{i-1/2,k+1/2}}{2\Delta}-\alpha_{n,l}\frac{\Delta_x}{2\Delta x}q_U(\alpha_{n,l}))^j_{i+3/2,k+1/2}\\&\quad=\frac{\Delta_x^2}{4\Delta x^2}\big(U^j_{i,k}+U^j_{i-1,k+1}+U^j_{i+2,k}+U^j_{i+1,k+1}\big),\end{aligned} \tag{4.10}$$

$$\begin{aligned}&\frac{(q_D(\alpha_{n,l}))^j_{i-1/2,k-1/2}-(q_D(\alpha_{n,l}))^j_{i-5/2,k-1/2}}{2\Delta}-\alpha_{n,l}\frac{\Delta_x}{2\Delta x}q_D(\alpha_{n,l}))^j_{i-5/2,k-1/2}\\&\quad=\frac{\Delta_x^2}{4\Delta x^2}\big(D^j_{i,k}+D^j_{i-1,k-1}+D^j_{i-2,k}+D^j_{i-3,k-1}\big).\end{aligned} \tag{4.11}$$

Solving for $q_U(\alpha_{n,l}))^j_{i+1/2,k+1/2}$, $q_D(\alpha_{n,l}))^j_{i-1/2,k+1/2}$ from the above equations and inserting

them into (4.1) and (4.2), we get

$$\left(1-\frac{\Delta^2}{4\Delta x^2}\Delta_x^2\right)U_{i,k}^j$$
$$=\left(1+\frac{\Delta^2}{4\Delta x^2}\Delta_x^2\right)U_{i+1,k-1}^j+\frac{\Delta^2}{4\Delta x^2}\Delta_x^2\left(U_{i+3,k-1}^j+U_{i+2,k}^j\right)+\Delta z\cdot v_{k-1/2}^j p_{i+1/2,k-1/2}^j$$
$$-\Delta z\cdot\sum_{l=1}^{n}a_{n,l}\left(1-\alpha_{n,l}\frac{\Delta}{\Delta x}\Delta_x\right)(q_U(\alpha_{n,l}))_{i+5/2,k-1/2}^j, \tag{4.12}$$

$$\left(1-\frac{\Delta^2}{4\Delta x^2}\Delta_x^2\right)D_{i,k}^j$$
$$=\left(1+\frac{\Delta^2}{4\Delta x^2}\Delta_x^2\right)D_{i-1,k-1}^j+\frac{\Delta^2}{4\Delta x^2}\Delta_x^2\left(D_{i-2,k}^j+D_{i-3,k-1}^j\right)-\Delta z\cdot v_{k-1/2}^j p_{i-1/2,k-1/2}^j$$
$$+\Delta z\cdot\sum_{l=1}^{n}a_{n,l}\left(1+\alpha_{n,l}\frac{\Delta}{\Delta x}\Delta_x\right)(q_U(\alpha_{n,l}))_{i-5/2,k-1/2}^j. \tag{4.13}$$

The numerical computation begins at the surface $z=0$ and advances in the positive z-direction. At each layer z, D and q_D are solved from $t=z$ to $t=T$ with the initial-time conditions (3.8), U and q_U are solved from $t=T$ to $t=z$ with the large-time conditions (3.9) or (3.12). The details of the algorithm are as follows:

Step 1.

When $k=0$:

Compute U, D, p at $k=0$ by conditions (3.7);

Compute $v_0^j=-2U_{0,0}^j$;

Step 2.

When $k>0$, compute U, D, q_U, q_D, p and v at this layer:

a. Prediction

Use first-order scheme

$$\frac{p_{i,k}^j-p_{i,k-1}^j}{\Delta}=\frac{U_{i,k-1}^j-D_{i,k-1}^j}{2}, \tag{4.14}$$

to pre-estimate $p_{i,k}^j$;

Let $v_{k-1/2}^j=v_{k-1}^j$;

Compute U and q_U by (4.12) and (4.4) with conditions (3.9) or (3.12);

Compute D and q_D by (4.13) and (4.5) with conditions (3.8);

b. Correction

Let $v_k^j=-2U_{k,k}^j$, $v_{k-1/2}^j=(v_{k-1}^j+v_k^j)/2$;

Compute $p_{i,k}^j$ by (4.3);

Compute U and q_U by (4.1) and (4.4) with conditions (3.9);

Compute D and q_D by (4.2) and (4.5) with conditions (3.8);

Use the new $U_{k,k}^j$ to correct $v_k^j=-2U_{k,k}^j$;

Step 3.

Let $k=k+1$, repeat step 2 until a predetermined depth Z.

The above algorithm has second-order accuracy. U, D, and p are solved at integer grid points (i, k) and q_U and q_D are solved at half integer grid points $(i + \frac{1}{2}, k + \frac{1}{2})$.

In the numerical implementation, we find that the above inversion algorithm for the one-way wave equations has several advantages. First, the derived coupled one-way wave equations have definite physical meanings. Second, for any n, all of the high order approximate equations for q_U and q_D are first-order partial differential equations. This avoids the difficulty of solving higher order partial differential equations which is required by other wave splitting algorithms. Third, all of the equations for the auxiliary functions $q_U(\alpha_{n,l})$ and $q_D(\alpha_{n,l})$ satisfy the same type of equation and they are fully uncoupled. Thus, q_U or q_D can be found by calling the same subroutine with different coefficients α in numerical computations. Fourth, although q_U or q_D appears to be a four-dimensional function $(l; t, x, z)$, by careful analysis, only a two-dimensional array is needed, one dimension for x and another for l (from 1 to n). Since n does not exceed 20 in numerical computations, memory storage is saved.

5. ITERATIVE ALGORITHM

Numerical results illustrate that the potentials reconstructed by solving the inverse problem for the system of coupled one-way wave equations do not have enough accuracy. This is due to several reasons. First, the system of coupled one-way wave equations are an approximation to the original equation in some sense (see discussion in Section 2). Second, the response $h(t, x)$ used in inversion is not the response of a forward problem for the system of coupled one-way wave equations; thus we cannot expect to obtain an accurate potential v from h by simply solving the coupled system (3.6). Third, the large-time conditions (3.9) are not accurate (see Remark 2 in Section 3). In this section we construct an iterative algorithm to improve the inversion accuracy.

For the potential $v(x, z)$, a response can be obtained by solving the direct problem for the wave equation (1.1),

$$h(t, x) = (\mathcal{A}v)(t, x). \tag{5.1}$$

Similarly, by solving the direct problem for the system of coupled one-way wave equations (3.1), another response can be obtained,

$$h_S(t, x) = (\tilde{\mathcal{A}}v)(t, x). \tag{5.2}$$

Generally, $\mathcal{A}^{-1}$ is an unbounded operator, but numerical experiments show that the inverse problem for (5.2) is well-posed. If $h_S(t, x)$ is known, we can obtain the potential by solving a well-posed inverse problem,

$$v(x, z) = \left(\tilde{\mathcal{A}}^{-1}h_S\right)(x, z). \tag{5.3}$$

Since

$$h_S(t, x) = h(t, x) - (h(t, x) - h_S(t, x)), \tag{5.4}$$

i.e.,

$$h_S(t, x) = h(t, x) - (\mathcal{A}v - \tilde{\mathcal{A}}v)(t, x). \tag{5.5}$$

Given an approximate potential $\bar{v}(x, z)$, $h_S(t, x)$ can be approximately represented as

$$h_S(t, x) \approx h(t, x) - (\mathcal{A}\bar{v} - \tilde{\mathcal{A}}\bar{v})(t, x). \tag{5.6}$$

From the above heuristic discussion, we construct an iterative algorithm as follows:

Step 1. For $m = 0$, let $h_I^0 = h(t, x)$, where m is the index of iteration;

Step 2. For the known response $h_I^m(t, x)$, solve the inverse problem for the system of coupled one-way wave equations (3.6)–(3.8), (3.12), and (3.10),

$$v^m(x, z) = \left(\tilde{\mathcal{A}}^{-1} h_I^m\right)(x, z); \tag{5.7}$$

Step 3. Compute the direct problem for the wave equation

$$h_W^{m+1}(t, x) = (\mathcal{A}v^m)(t, x) \tag{5.8}$$

and the one-way wave equations,

$$h_S^{m+1}(t, x) = (\tilde{\mathcal{A}}v^m)(t, x); \tag{5.9}$$

Step 4. If

$$\varepsilon = \left\| h(t, x) - h_W^{m+1}(t, x) \right\| \tag{5.10}$$

is small enough, stop the iteration; otherwise, go to step 5;

Step 5. According to (5.6), compute

$$h_I^{m+1}(t, x) = h(t, x) - \left(h_W^{m+1}(t, x) - h_S^{m+1}(t, x)\right); \tag{5.11}$$

Step 6. Let $m = m + 1$; go to step 2.

Remark. In the iteration,

$$h_I^{m+1} = h(t, x) - \left(h_W^{m+1} - \tilde{\mathcal{A}}\tilde{\mathcal{A}}^{-1} h_I^m\right). \tag{5.12}$$

To simplify the computation, if we assume

$$\mathcal{I} = \tilde{\mathcal{A}}\tilde{\mathcal{A}}^{-1}, \tag{5.13}$$

then

$$h_I^{m+1} = h(t, x) - \left(h_W^{m+1} - h_I^m\right) = h(t, x) - \left(\mathcal{A}v^m - h_I^m\right). \tag{5.14}$$

Therefore, we do not need to solve the direct problem for the one-way wave equations, and some computations are saved. Here we point out that (5.13) is not always true, because, first, the domain of $\tilde{\mathcal{A}}^{-1}$ is not necessarily equal to the range of $\tilde{\mathcal{A}}$, second, as pointed out in Section 3, the large-time conditions used for computing $\tilde{\mathcal{A}}^{-1}$ (either (3.9) or (3.12)) are approximate conditions.

6. NUMERICAL TESTS AND RESULTS

In [13, 28], several numerical tests are presented for the cases, $n = 1, 2$. In this paper, we construct the difference scheme for high-order approximations (arbitrary n) for the one-way wave equations and use the iterative algorithm to get improved inversion results. Numerical experiments are performed on several examples, and the computed results show that this method is very effective for certain potential models.

We define

$$\text{maximum error} = \frac{\max_{j,k} \left| v_k^j - \bar{v}_k^j \right|}{\max_{j,k} \left| v_k^j \right|}, \tag{6.1}$$

$$\text{average error} = \frac{\sum_{j,k} \left| v_k^j - \bar{v}_k^j \right|}{N_x N_z \cdot \max_{j,k} \left| v_k^j \right|}, \tag{6.2}$$

where v is a given potential function and the $\bar{v}$ are the results of the inversion method. In all the examples, conditions (3.12) are used instead of (3.9). For simplicity, we use periodic boundary conditions in x.

EXAMPLE 1. The given potential (Fig. 3a) is

$$v(x,z) = \begin{cases} \frac{1}{2}\left[1 + \cos\frac{(10x-15)\pi}{12}\right]\sin\frac{(30z-11)\pi}{8}, & x \in \left[\frac{3}{10}, \frac{27}{10}\right], z \in \left[\frac{11}{30}, \frac{19}{30}\right], \\ 0, & \text{otherwise.} \end{cases} \tag{6.3}$$

It is a smooth function, and the variation along the x-direction is slower than that of the z-direction. For such a "nice" function we can obtain remarkably good inversion results. Here, we use three different approximations ($n = 2, 5, 10$) and show the errors for their first 20 iterations in Fig. 2. In all the numerical experiments, $x \in [0, 3]$, $z \in [0, 1]$, $t \in [0, 4]$, and the grid numbers in the x, z, and t directions are respectively $N_x = 40$, $N_z = 80$, and $N_t = 160$, with $\Delta x = 0.075$, $\Delta = 0.0125$. Figure 3 shows the results for $n = 10$.

From Fig. 2 we see that the inversion accuracy for $n = 5, 10$ is much better than for $n = 2$. Further, we see that for large n, the error of inversion decreases more quickly than for small

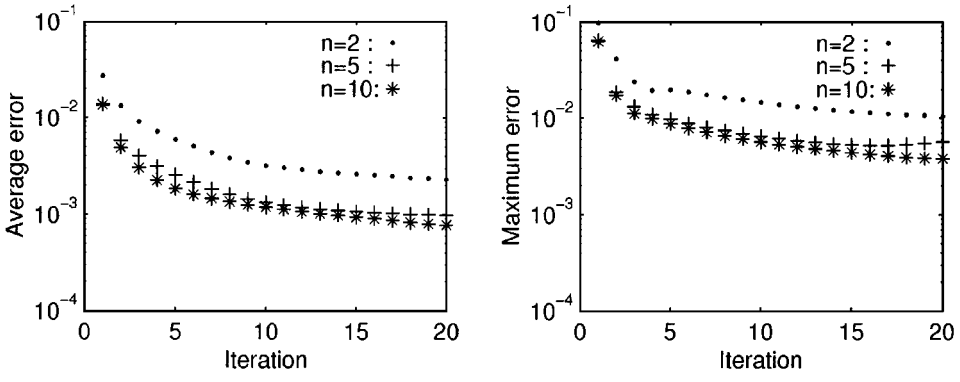

FIG. 2. The error of the inversions for different approximate one-way wave equations: left, the average error; right, the maximum error.

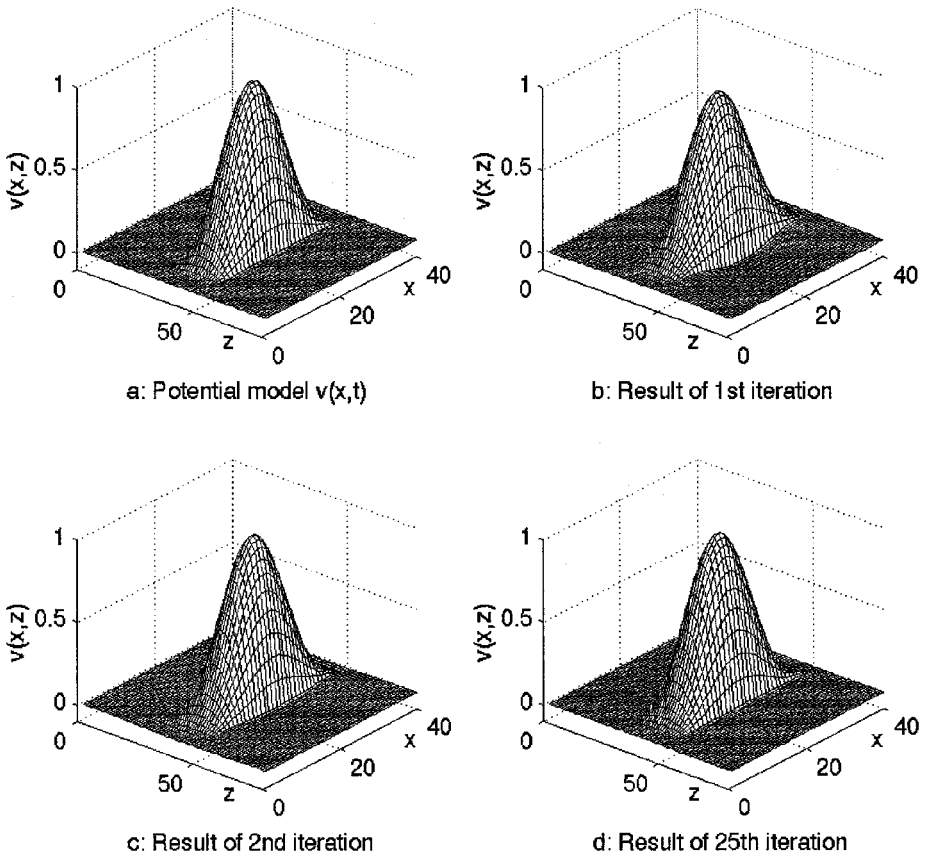

FIG. 3. (a) the potential in example 1; (b–d) the inversion results for example 1 ($n = 10$): (b) the inversion result of the first iteration; (c) the inversion result of the second iteration; (d) the inversion result of the 25th iteration.

n during iterations. So we conclude that using higher order approximations for the one-way wave equations improves inversion results.

To test the numerical stability of the inversion algorithm, Gaussian random noise was added to the reflection response $h(t, x)$; see Fig. 4a. The ratio of noise to signal is $\|n(t, x)\|_{L_2}/\|h(t, x)\|_{L_2} = 14.4\%$. The noisy reconstruction is shown in Fig. 4b. The average error and the maximum error are 0.0197 and 0.0993, respectively. Comparing with the original potential function in Fig. 3a, we see that the inversion algorithm does not fall apart even with large amounts of additive noise.

EXAMPLE 2. Let

$$v^*(x, z) = \begin{cases} \left[1 + \cos\frac{(10x-15)\pi}{12}\right] \cdot \sin\frac{(30z-11)\pi}{8}, & x \in \left[\frac{3}{10}, \frac{27}{10}\right], z \in \left[\frac{11}{30}, \frac{19}{30}\right], \\ 0, & \text{otherwise}, \end{cases} \tag{6.4}$$

and

$$v(x, z) = \begin{cases} v^*(x, z), & \text{if } v^* < 1, \\ 1, & \text{if } v^* \geq 1. \end{cases} \tag{6.5}$$

Note that $v(x, z)$ is a platform-like function; see Fig. 5a.

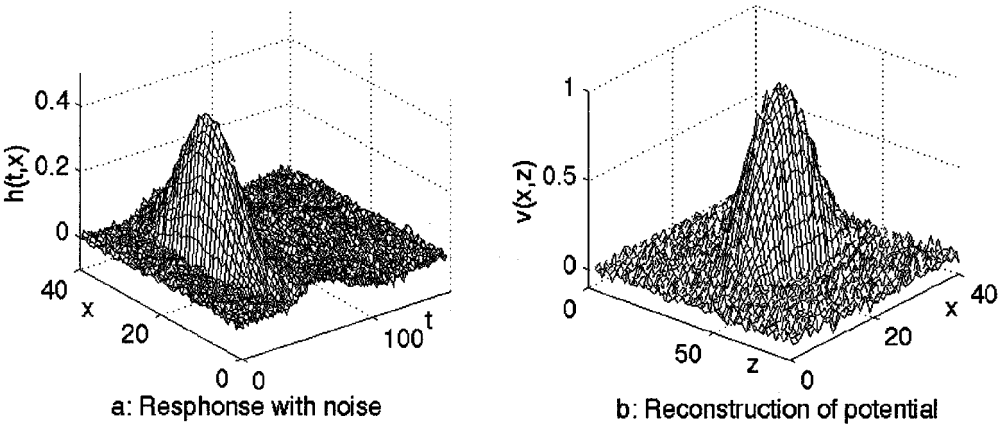

FIG. 4. (a) Noise-contaminated response; (b) reconstructed potential.

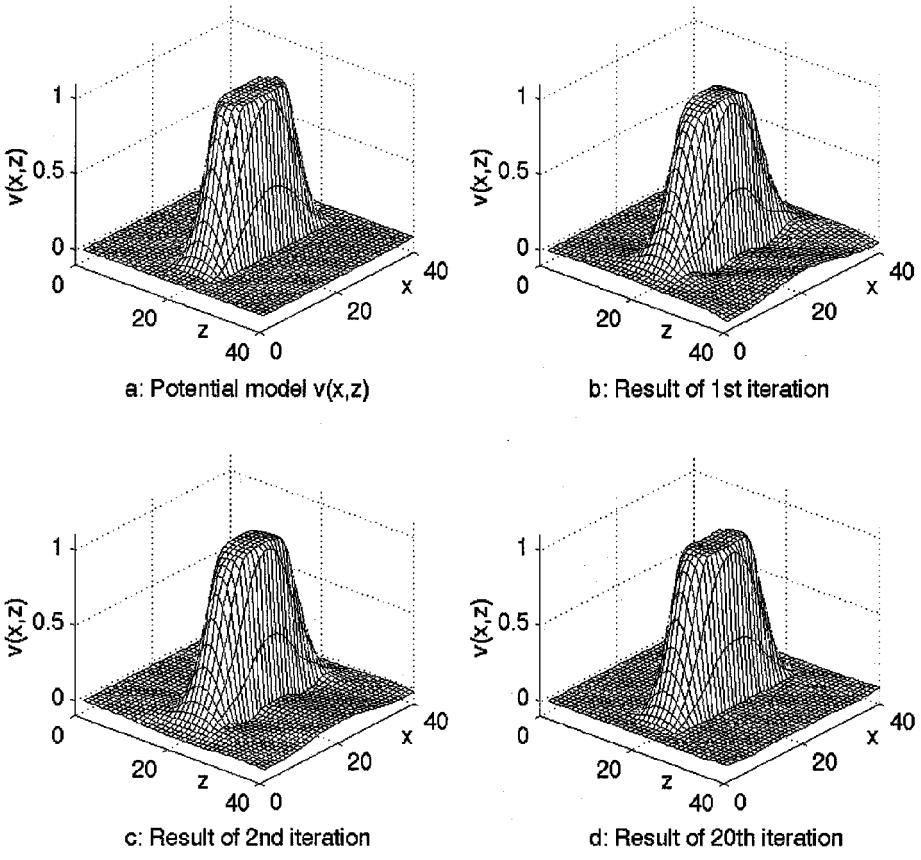

FIG. 5. (a) the potential in Example 2; (b–d) the inversion results for Example 2 ($n = 10$): (b) the inversion result of the first iteration; (c) the inversion result of the second iteration; (d) the inversion result of the 20th iteration.

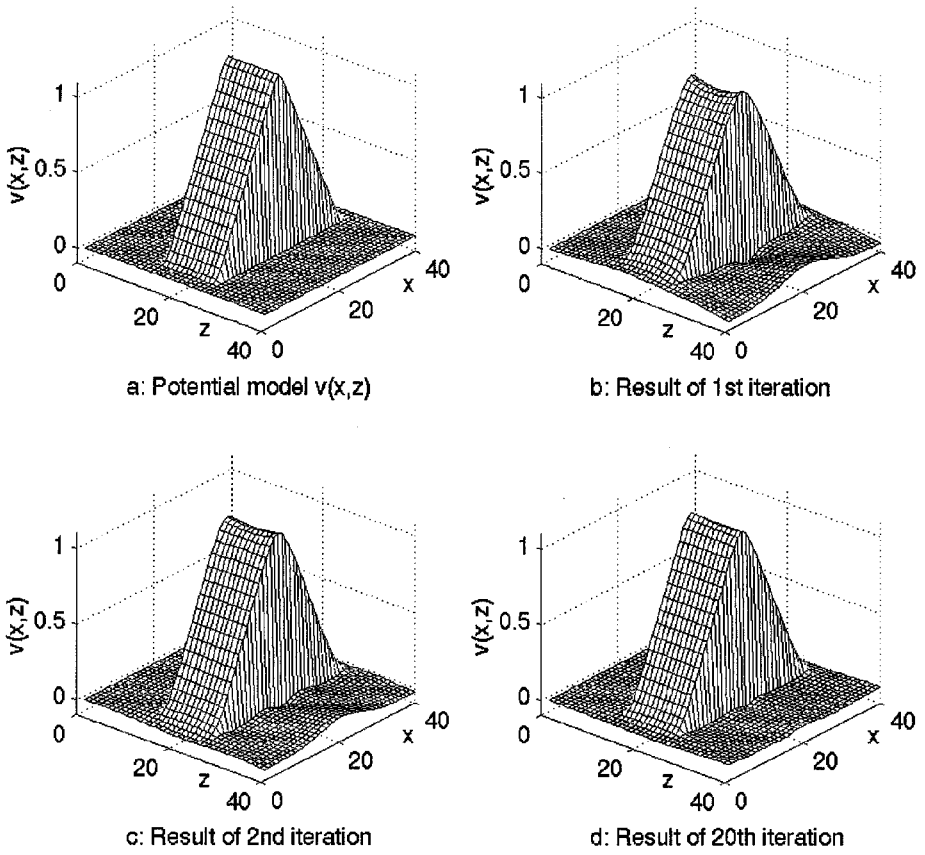

FIG. 6. (a) the potential in Example 3; (b–d) the inversion results for example 3 ($n = 10$): (b) the inversion result of the first iteration; (c) the inversion result of the second iteration; (d) the inversion result of the 20th iteration.

The inversion results are shown in Fig. 5, where $x \in [0, 3]$, $z \in [0, 1]$, and $t \in [0, 2.25]$, the numbers of grid points are $N_x = 40$, $N_z = 40$, and $N_t = 45$, and $\Delta x = 0.075$, $\Delta = 0.025$, and $n = 10$. It was reported in [22] that for such a potential which drops off rapidly to zero in the deep part, the linearized reconstruction, based on the Born approximation, always has a "tail" which goes to zero very slowly. This is due to the multiple reflection in the response which is considered as the primary reflection in the linearized inversion. From Fig. 5, we see that the reconstructed potential using the layer-stripping algorithm is nearly perfect. The central "plateau" is well reconstructed and no "tail" is found in the deep part. The average error and the maximum error for the final reconstruction are 0.00264 and 0.0338, respectively.

EXAMPLE 3. The given potential (see Fig. 6a) is

$$v(x,z) = \begin{cases} \frac{10x-3}{10}, & x \in [0.3, 1.5], z \in [0.35, 0.65], \\ \frac{27-10x}{10}, & x \in [1.5, 2.7], z \in [0.35, 0.65], \\ 0, & \text{otherwise.} \end{cases} \tag{6.7}$$

For such a potential, we can get good inversion results, and the discontinuity along the z direction can be well reconstructed; see Fig. 6. In computing, $x \in [0, 3]$, $z \in [0, 1]$, $t \in [0, 2.25]$, $N_x = 40$, $N_z = 40$, $N_t = 45$, and $\Delta x = 0.075$, $\Delta = 0.025$, $n = 10$.

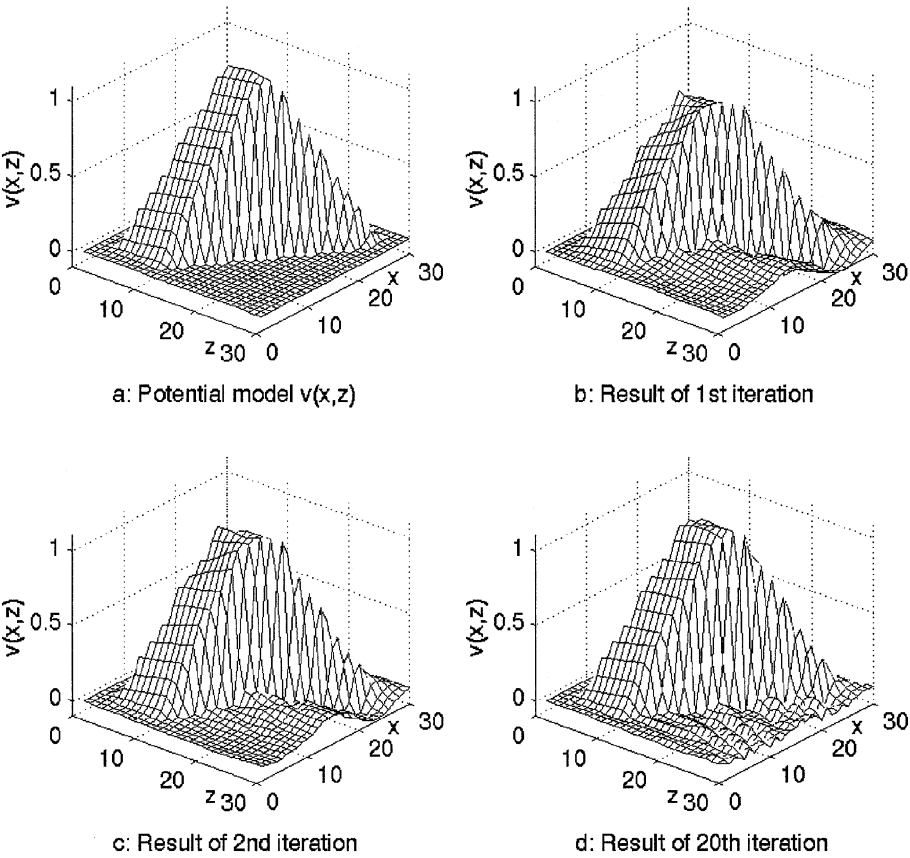

FIG. 7. (a) the potential in Example 4; (b–d) the inversion results for Example 4 ($n = 10$): (b) the inversion result of the first iteration; (c) the inversion result of the second iteration; (d) the inversion result of the 20th iteration.

EXAMPLES 4 AND 5. For the last two examples, the given potentials are obtained by rotating the potential in Example 3 by 15° and 30°, respectively. See Fig. 7a and Fig. 8a. In both examples, the potentials are discontinuous along the z and x directions. The inversion results are shown in Figs. 7 and 8, and the errors, comparing with that of Example 3 can be seen in Fig. 9. Numerical experiments show that the inversion becomes more difficult when the slope becomes larger. Even for a slope-like potential with small angle, the inversion will be divergent after several iterations. But if we stop the iteration earlier, reasonably good results can be obtained. In computing for both examples, $x \in [0, 3]$, $z \in [0, 1]$, $t \in [0, 2.33]$, $N_x = 30$, $N_z = 30$, $N_t = 35$, $\Delta x = 0.1$, $\Delta = 0.033$, and $n = 10$.

7. CONCLUSIONS

We have developed a method for solving the 2D potential inverse problem. By using the wave splitting technique, the ill-posed inverse problem for the higher dimensional wave equation is naturally regularized, so that it can be solved by a layer-stripping algorithm. The iterative method proposed in Section 5 remarkbly improves the inversion accuracy. From the numerical experiments, we see that this method is very effective for potential models

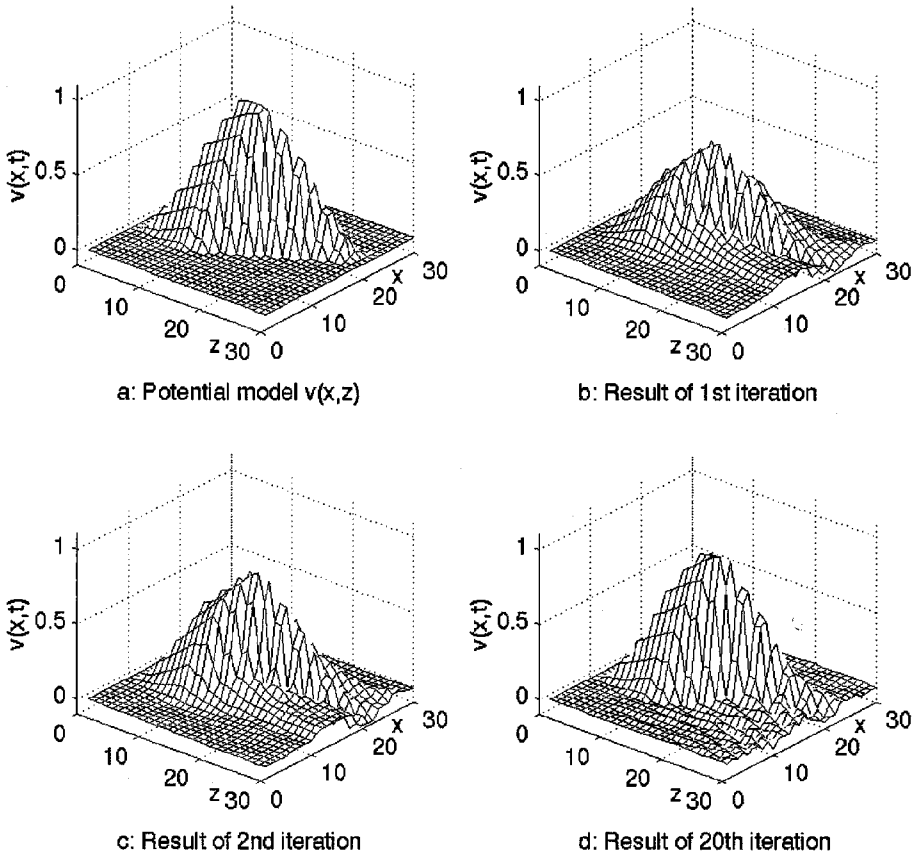

FIG. 8. (a) the potential in Example 5; (b–d) the inversion results for Example 5 ($n = 10$): (b) the inversion result of the first iteration; (c) the inversion result of the second iteration; (d) the inversion result of the 20th iteration.

whose variation along the reference spatial direction of z, is greater than that of lateral directions. This method can also be generalized to solve the 3D case and other kinds of propagation inverse problems. For example, the coefficient inverse problem of the acoustic wave equation, whose corresponding inversion formulation is given in [26], may be solved

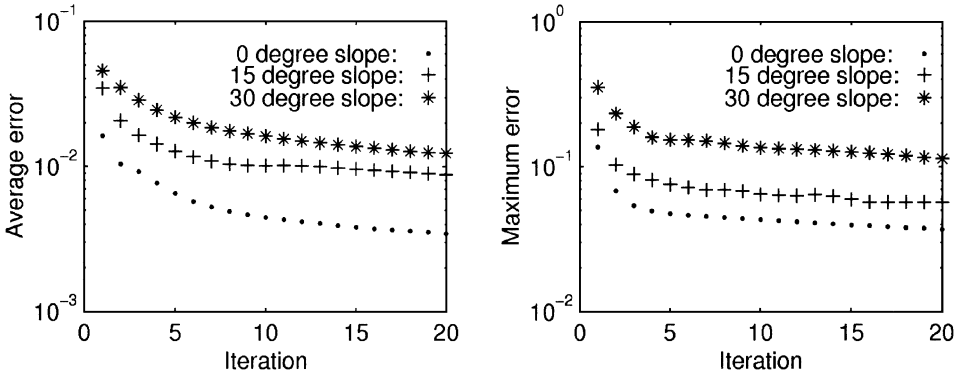

FIG. 9. The error of the inversions for different slope-like potentials: 0° slope (Example 3), "•"; 15° slope (Example 4), "+"; 30° slope (Example 5), "*." Left, the average error; right, the maximum error.

by this method. Concerning the case of nonimpulsive sources, an inversion method called characteristic band method has been developed in [30, 14] for the 1D problems, which can be generalized to the multidimensional cases.

APPENDIX: PROOF OF PROPOSITION 1

By the transformation $t = s/\sqrt{1-s^2}$, the left-hand side becomes

$$1 - \frac{\xi^2}{\pi}\int_{-1}^{1}\frac{\sqrt{1-s^2}}{1-\xi s}\,ds = 1 - \frac{\xi^2}{\pi}\int_{-1}^{1}\frac{\sqrt{1-s^2}}{1-\xi^2 s^2}\,ds = \frac{2}{\pi}\int_0^{\infty}\frac{1-\xi^2}{1+(1-\xi^2)t^2}\,dt.$$

Let $1-\xi^2 = re^{i\theta}$, $r \geq 0$, $\theta \in [0, 2\pi)$ and $q = r^{1/2}t$, then we have

$$\begin{aligned}
1 - \frac{\xi^2}{\pi}\int_{-1}^{1}\frac{\sqrt{1-s^2}}{1-\xi^2 s^2}\,ds &= \frac{2r^{1/2}}{\pi}\int_0^{\infty}\frac{e^{i\theta}}{1+e^{i\theta}q^2}\,dq \\
&= \frac{2r^{1/2}}{\pi}\,e^{i(\theta/2)}\lim_{a\to+\infty}\int_0^{ae^{i(\theta/2)}}\frac{dZ}{1+Z^2} \\
&= \frac{2r^{1/2}}{\pi}\,e^{i(\theta/2)}\lim_{a\to+\infty}\arctan(Z)\Big|_{Z=0}^{ae^{i(\theta/2)}} \\
&= \frac{r^{1/2}}{\pi i}\,e^{i(\theta/2)}\lim_{a\to+\infty}\left[\ln\left|\frac{i-Z}{i+Z}\right| + i\cdot\mathrm{Arg}\frac{i-Z}{i+Z}\right]\Big|_{Z=0}^{ae^{i(\theta/2)}} \\
&= r^{1/2}\,e^{i(\theta/2)} = \sqrt{1-\xi^2}.
\end{aligned}$$

This completes the proof.

ACKNOWLEDGMENT

We are very grateful to Dr. John A. Pelesko for carefully reading and rewriting this paper.

REFERENCES

1. G. Bao, Inverse problems in partial differential equations, in *Numerical Methods in Applied Sciences*, edited by W. Cai, Z. Shi, C. Shu, and J. Xu (Science, New York, 1996).
2. A. J. Berkhout, Steep dip finite-difference migration, *Geophys. Prosp.* **27**, 196 (1979).
3. K. Bube and R. Burridge, The one-dimensional inverse problem of reflection seismology, *SIAM Rev.* **25**, 497 (1983).
4. R. Burridge, The Gel'fand–Levitan, the Marchenko, and the Gopinath–Sondhi integral equations of inverse scattering theory, regarded in the context of inverse impulse–response problems, *Wave Motion* **2**, 305 (1980).
5. J. F. Claerbout and S. M. Doherty, Downward continuation of moveout corrected seismograms, *Geophysics* **37**, 741 (1976).
6. J. K. Cohen and N. Bleistein, Velocity inversion procedure for acoustic waves, *Geophysics* **44**, 1077 (1979).
7. X. L. Dou, *Potential inversion for an 2-D wave equation*, Ph.D. thesis, Institute of Computational Mathematics and Scientific/Engineering Computing, Chinese Academy of Sciences, June 1994. [Chinese]
8. B. Enquist and A. Majda, Radiation boundary conditions for acoustic and elastic wave calculation, *Comm. Pure. Appl. Math.* **32**, 313 (1979).
9. L. Fishman, Exact and approximate solutions of the Helmholtz, Weyl composition equation in scale wave propagation, *Wave Motion* **14**, 205 (1991).

10. V. Isakov, Uniqueness and stability in multi-dimensional inverse problems, *Inverse Problems* **9**, 305 (1993).
11. C. S. Morawetz and G. Kriegsmann, The calculations of an inverse potential problem, *SIAM J. Appl. Math.* **43**, 844 (1983).
12. M. M. Sondhi and B. Gopinath, Determination of vocal-tract shape from impulse response at lips, *J. of Acoust. Soc. of America* **49**, 1867 (1971).
13. H. Song and G. Q. Zhang, Potential inversion of the two-dimensional plasma wave equation, *Inverse Problems* **10**, 464 (1994).
14. H. B. Song, Z. T. Ma, and G. Q. Zhang, Simutaneous inversion of layered compressional velocity and shear velocity by using plane wave seismogram, *Sci. China Ser. D* **39**(6), 618 (1996).
15. R. H. Stolt, Migration by fourier transform, *Geophysics* **43**, 23 (1978).
16. R. H. Stolt and A. K. Benson, *Seismic Migration* (St. Catherine, Bruges, 1986).
17. W. Symes, Inverse boundary value problems and a theorem of Gel'fand and Levitan, *J. Math. Anal. Appl.* **71**, 379 (1979).
18. A. Tarantola, *Inverse Problem Theory* (Elsevier, Amsterdam, 1989).
19. D. L. Wang and G. Q. Zhang, Convergence of difference methods for inverse problems of a one-dimensional hyperbolic systems of first order, *J. Comput. Math.* **6**(3), 226 (1988).
20. V. H. Weston, Factorization of the wave equation in higher dimension, *J. Math. Phys.* **28**, 1061 (1987).
21. A. E. Yagle and B. C. Levy, Layer stripping solutions of multidimensional inverse scattering problems, *J. Math. Phys.* **27**, 1701 (1986).
22. A. E. Yagle and P. Raadhakrishan, Numerical performance of layer stripping algorithms for 2-d inverse scattering problem, *Inverse Problems* **8**, 645 (1992).
23. G. Q. Zhang, High order approximation of one-way wave equations, *J. Comput. Math.* **3**, 90 (1985).
24. G. Q. Zhang, A new algorithm for finite-difference migration of steep dips, *Geophysics* **53**, 167 (1988).
25. G. Q. Zhang, On an inverse problem for 1-dimensional wave equation, *Sci. China Ser. A* **32**, 257 (1989).
26. G. Q. Zhang, Square-root operator and its applications in numerical solution of some wave problems, in *Proceeding of the First China-Japan Seminar on Numerical Mathematics, Beijing, 1992.*
27. G. Q. Zhang, System of coupled equations for upcoming and downgoing waves, *Acta Math. Appl. Sinica* **16**, 251 (1993). [Chinese]
28. G. Q. Zhang and X. L. Dou, Numerical solution of 2-d potential inverse problems, in *Proc. of the 2nd Inter. Symp. on Inverse Problems-ISIP'94, Paris, 1994*, edited by Balkema, Rotterdam, and Brookfield. p. 467.
29. Y. Zhang, *Study on the Inverse Problems in Wave Equations*, Ph.D. thesis, Institute of Computational Mathematics and Scientific/Engineering Computing, Chinese Academy of Sciences, June 1996. [Chinese]
30. Y. Zhang and G. Q. Zhang, The characteristic band method for acoustic impedance inversion, *Math. Numer. Sinica* **20**(4), 385 (1998). [Chinese]